GEOMAGNETIC EFFECTS OF SLOPING AND SHELVING DISCONTINUITIES OF EARTH CONDUCTIVITY†

F. WALTER JONES* AND ALBERT T. PRICE‡

The surface effects on electric and magnetic variations arising from interfaces in three two-dimensional conductivity models are compared in detail for four frequencies. It is found that the horizontal extent of the surface effects greatly depends on the dimensions of the different structures relative to the skin depths at the frequencies used. Also, a fundamentally important difference is revealed between H-polarization and E-polarization problems in that the apparent resistivity computed on the surface near the contact is discontinuous and changes abruptly in the H-polarization case, whereas for E-polarization the apparent resistivity is continuous and changes gradually across the contact.

INTRODUCTION

In recent work by Jones and Price (1969, 1970a), we considered the perturbation of an alternating geomagnetic field by an abrupt vertical discontinuity in conductivity and determined in detail the magnetic field and current distributions throughout the composite conductor. The technique applied was that of solving the equations and boundary conditions by means of the Gauss-Seidel iteration method. Our model was two-dimensional with a vertical contact between the two regions of different conductivity (model 1 in Figure 1). Two polarization cases (H-polarization, where the magnetic field is parallel to the strike, and E-polarization, where the electric field is parallel to the strike) were solved. We have now extended our technique to consider two more models and have made comparisons of the surface effects of the discontinuities for the different models.

THE MODELS

The coordinate system and the three models are shown in Figure 1.

Model 1 is the original model (Jones and Price, 1970a), which consists of a semi-infinite conduct-

ing region composed of two quarter-spaces of different conductivity.

Model 2 is one with a sloping contact between the two regions of the conductor. The slope is 45 degrees and, rather than being continuous, is actually stepped, since the numerical method involves the solution of equations and boundary conditions over a uniform square grid. Model 2 is therefore termed the "step" model.

Model 3 is called the "shelf" model. In it, a shelf-type contact exists between the two regions of different conductivity in the conducting half-space.

In all three models, the grid spacing is taken as 1.5 km. The mesh is square and contains 1681 grid points (41×41), modeling, therefore, a cross-section 60 km square. The surface of the earth is taken as the center horizontal row of grid points, and the surface contact between the two conducting regions is the center point of this line. For model 2, the steps are one grid spacing in height (1.5 km) and one grid spacing in width (1.5 km). In model 3, the depth from the surface to the shelf is 4 grid spacings (6.0 km) and the length of the shelf is 11 grid spacings (16.5 km).

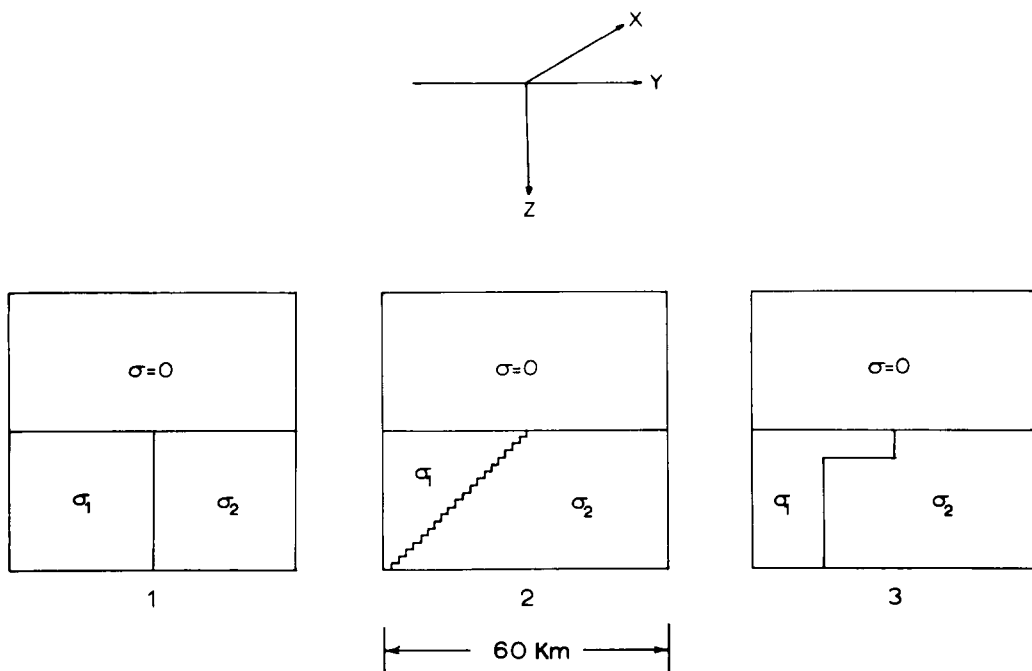These models have some of the features of an

FIG. 1. The coordinate system and the three models used: (1) the vertical contact model, (2) the step model, (3) the shelf model.

ocean-continental boundary, but neither model 2 nor model 3 accurately approximates an actual continental shelf, since the ocean depth over the actual shelf is much less and the width of the shelf is much greater than those of the models. Since a square grid is used, we cannot obtain a depth-to-width ratio which represents correctly the true continental shelf. However, by considering the models used, we can gain some understanding of the various effects and can apply what we learn to the actual situation.

The conductivities chosen were $\sigma_1 = 4.0$ mho-m^{-1} (resistivity = 0.25 ohm-m) and $\sigma_2 = 10^{-3}$ mho-m^{-1} (resistivity = 1000 ohm-m). These are approximate conductivities for sea water and the continental crust. The frequencies investigated were 0.01 hz (100 sec period), 0.003 hz (approximately 5.6 minute period), 0.001 hz (approximately 16.7 minute period), and 0.0003 hz (approximately 55.6 minute period). The skin depths for the two conductivities at these frequencies are given in Table 1.

NUMERICAL FORMULATION OF THE PROBLEM

The equations to be solved in all regions for both cases have the form

$$\nabla^2 F = i\eta^2 F, \quad \text{(Jones and Price 1970a)},$$

with the appropriate value of η (a function of the conductivity) inserted; F represents either H_x or E_x.

If $F = f + ig$, $\nabla^2 F = \nabla^2(f + ig) = \nabla^2 f + i\nabla^2 g$ and $i\eta^2 F = i\eta^2(f + ig) = i\eta^2 f - \eta^2 g$. Equating real and imaginary parts, we obtain $\nabla^2 f = -\eta^2 g$ and $\nabla^2 g = \eta^2 f$.

These two equations are replaced by corresponding finite difference equations, which are then solved simultaneously for each point on the mesh by finite difference methods. The methods also take into account the boundary conditions (Jones and Price 1970a).

THE SURFACE EFFECTS

We shall consider the three models in detail by comparing the surface values of the fields and the components which may be calculated for the H-polarization and E-polarization cases. Also the phases of the components and various ratios are considered.

H-polarization

For H-polarization, H_x is constant along the surface (Jones and Price 1970a). Also, for both

Table 1. Skin depths of the conductors for
the four frequencies used

	0.01 hz	0.003 hz	0.001 hz	0.0003 hz
$\sigma_1 = 4.0$ mho-m^{-1}	2.52 km	4.59 km	7.96 km	14.53 km
$\sigma_2 = 10^{-3}$ mho-m^{-1}	159.2 km	290.6 km	503.3 km	918.8 km

H-polarization and E-polarization, E_z along the
surface is zero (Jones and Price, 1970a). There-
fore, the only component calculated is E_y, the
horizontal component of the electric field. Since
H_x is constant, we may also find E_y/H_x; and ρ_A,
the apparent resistivity, may be calculated for this
polarization. The phase of the horizontal com-
ponent of the electric field (ϕ_{E_y}) is computed along
the surface. The phase of E_y is calculated relative
to the phase at the end point over the region of
lower conductivity.

In Figure 2, the amplitude of E_y, the phase of
$E_y (\phi_{E_y})$, and ρ_A are plotted along the surface for
the 3 models for the 4 frequencies considered in
Table 1.

From Figure 2, we can see that E_y is discon-
tinuous over the abrupt change of conductivity at
the surface. Since H_x is constant along the surface
for this polarization, E_y/H_x is of the same form as
E_y; and ρ_A is also discontinuous at the contact as
shown.

A remarkable feature of the diagrams for ρ_A is
that this "apparent resistivity" sharply decreases
(i.e. the apparent conductivity *increases*) as the
interface is approached from the more highly
conducting ("seaward") side, and that ρ_A in-
creases (though less remarkably) as the interface
is approached from the "landward" side. Also,
for the longer period variations, ρ_A is smaller
(i.e., the apparent conductivity is *higher*) in the
area where the shelf is present. Moreover, ρ_A is
higher for the slower variations than for the faster
ones. This behavior would imply, according to
the usual magnetotelluric interpretation, an
increase of conductivity with depth in the neigh-
borhood of the shelf, whereas in models 2 and 3
there is actually a sudden decrease in the real
conductivity. The explanation of this curious
feature is that, in the case of H-polarization, the
currents are flowing parallel to the cross-sections
shown in Figure 1 and impinge against the inter-
face, where a surface charge is built up. The
amount of current needed to build up this surface
charge is negligibly small, but the electric field of
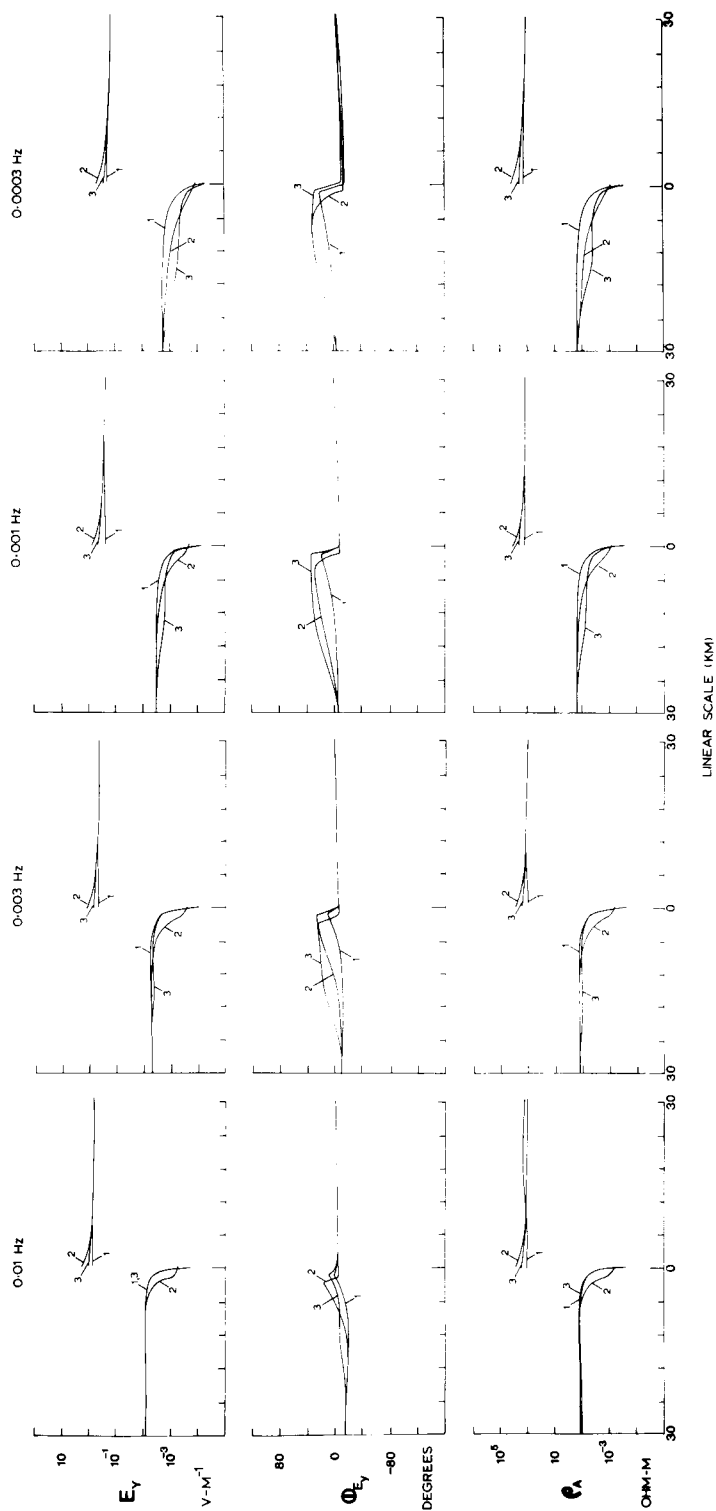this charge is quite important. It acts so as to

reduce E_y in the high conductivity region and so
as to increase E_y in the low conductivity region.
Consequently, the *apparent* resistivity, inferred
from the resultant E_y at the surface by use of the
Cagniard formula, is reduced near the interface
in the highly conducting region and increased in
the low conductivity region. This buildup of
surface charge on the interface is encountered in
all H-polarization problems (Jones and Price,
1970a). Most of the surface effects on the field
components are due to surface charge buildup and
consequently these field components cannot be
used directly in the usual magnetotelluric formula
to infer the actual conductivity distribution.

For the frequency 0.01 hz, E_y for models 1 and 3
is nearly the same. Since the skin depth in the
higher conducting region is considerably less than
the depth from the surface to the shelf of model 3,
the effect of the shelf is not seen at the surface.
However, the value of E_y for model 2 dips down
near the contact. In this case, the skin depth of
the higher conducting region is greater than the
depth of one step and nearly equal to the depth
of two steps. Therefore, the effects of the first
two steps appear at the surface. A similar situa-
tion is seen for ϕ_{E_y} and ρ_A for this frequency;
although the shelf (model 3) does slightly affect
the phase.

For the frequency 0.003 hz, the skin depth in
σ_1 is approximately equal to 3 step depths and the
effect of these steps is demonstrated by the varia-
tion of the components further from the contact
in model 2. Also, the skin depth is now beginning
to approach the depth of the shelf of model 3,
so that its presence is detected in E_y and ρ_A and is
strongly shown in ϕ_{E_y}.

For 0.001 hz, the skin depth is greater than 5
step heights of model 2; thus the influence of the
subsurface structure is being felt even further
from the surface contact. The skin depth is now
greater than the depth to the shelf of model 3
and the presence of the shelf is clearly indicated.
It may also be seen that there is some change in
the calculated functions for model 1 throughout
the 4 frequencies. The cutoff appears to become
less abrupt for the longer periods in this model,
but, as already stated, the surface effects are, in
the main, due to charge accumulated on the
boundary.

For 0.0003 hz, the subsurface structure is even
more evident. The skin depth in the higher con-

FIG. 2. H-polarization. E_y, ϕ_{E_y}, and ρ_A for the (1) vertical, (2) step, and (3) shelf models.

ducting region is 14.53 km at this frequency; consequently, about 10 steps will appreciably influence the surface effects of model 2. However, since the steps go deeper as the distance from the contact increases, the effect is different from that in model 3, where the depth to the shelf is fixed. It is seen that, at a distance from the surface contact, ϕ_{Ey} for the shelf and step models is the same but differs near the contact.

E-*polarization*

In the solution for the E-polarization, the amplitudes of E_x, H_y, and H_z are calculated, as well as their phases relative to the end point. Also, the ratios E_x/H_y and H_z/H_y and the apparent resistivity ρ_A are computed.

Figure 3 shows E_x, H_y, and H_z for the 3 models for the 4 frequencies considered. All 3 components are continuous across the discontinuity for this polarization (Jones and Price 1970b). For all 3 components, the surface contact of the discontinuity is most obvious for the highest frequency and becomes less prominent as the period increases. Also, we observe that H_y and H_z increase as the period increases.

For E_x, the effect of the step and shelf become apparent at 0.003 hz, and the two models are indistinguishable at 0.0003 hz.

Figure 3 indicates that across the surface of the discontinuity the variation of H_y is considerably less than the variation of H_z. Also, H_z and H_y are of the same order of magnitude. This behavior may be compared with the previous result obtained from model 1, when a conductivity ratio of 10 to 1 was used (Jones and Price, 1970a). In the previous work, the values of H_y and H_z were of the same order of magnitude and the variation of H_y and H_z across the contact was nearly the same size. Also, a comparison may be made with a buried inhomogeneity (Jones and Price, 1970b), for which the conductivity ratio was 100 to 1. In making these comparisons, we must take into account the difference in frequencies, which are lower for our present work than in our previous studies.

· Again in H_y and H_z the subsurface structure is evident at 0.003 hz, for which the skin depth in the higher conducting region is most nearly equal to the depth of the structures.

Figure 4 gives the ratios E_x/H_y, H_z/H_y, and the apparent resistivity ρ_A. Once more the sub-

surface structure is most apparent at 0.003 hz, a frequency for which the skin depth is about equal to 3 steps in model 2 and approaches the depth of the shelf of model 3. At 0.01 hz, there is an apparent minimum in H_z/H_y over the corner of the shelf in model 3. This becomes a local maximum at the lower frequencies. The apparent resistivity curves show that at the higher conducting end of the models, $\rho_A = 0.25$ ohm-m and at the lower conducting end, $\rho_A = 1000$ ohm-m. These values give the correct conductivities for calculations for a uniform earth at a great distance from the contact. The increase in ρ_A is apparent over the subsurface structures near the surface contact as the frequencies decrease from 0.01 hz to 0.0003 hz and the influence of the lower conducting region below the shelves becomes stronger at longer periods. In the case of E-polarization, there is no problem arising from charges accumulating on the interface, and the variations of ρ_A in the region of the interface are much as we would expect for each of the models considered.

The phase variations of the 3 calculated components $E_x(\phi_{Ex})$, $H_y(\phi_{Hy})$, and $H_y(\phi_{Hz})$ across the surface relative to the end point above the lower conducting medium are shown in Figure 5.

In ϕ_{Ex} there is a minimum on the higher conducting side of the surface contact. This minimum moves farther away from the contact and broadens as the period increases. The effects of the shelf and step contacts are strongly evident at 0.003 hz.

The variation of ϕ_{Hy} across the surface of the vertical discontinuity model 1 changes slightly for the 4 frequencies. For the two other models, the change in ϕ_{Hy} as the frequency goes from 0.01 hz to 0.0003 hz is considerable. The shelf and step models show their characteristic differences at all 4 frequencies but most obviously at 0.003 hz and 0.001 hz.

ϕ_{Hz} has a minimum on the higher conducting side of the surface contact in all 3 models. This minimum decreases as the period increases. At 0.01 hz, model 3 shows an abrupt step in ϕ_{Hz} over the subsurface corner of the shelf; ϕ_{Hz} for model 2 is much smoother. At 0.003 hz, the shelf corner of model 3 is again marked by a bump, while ϕ_{Hz} for model 2 changes even more smoothly. As the period increases, the effects of the subsurface structures remain but become less prominent.
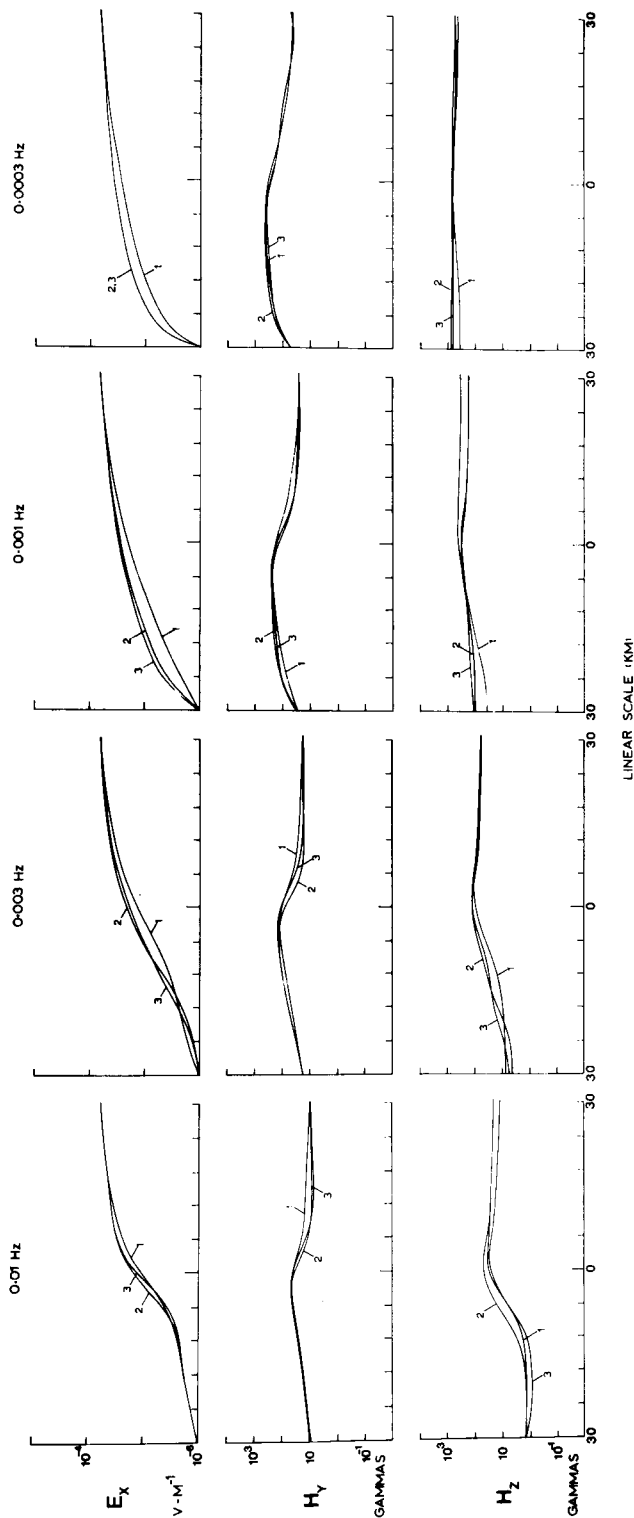
FIG. 3. E-polarization. E_x, H_y, and H_z for the (1) vertical, (2) step, and (3) shelf models.
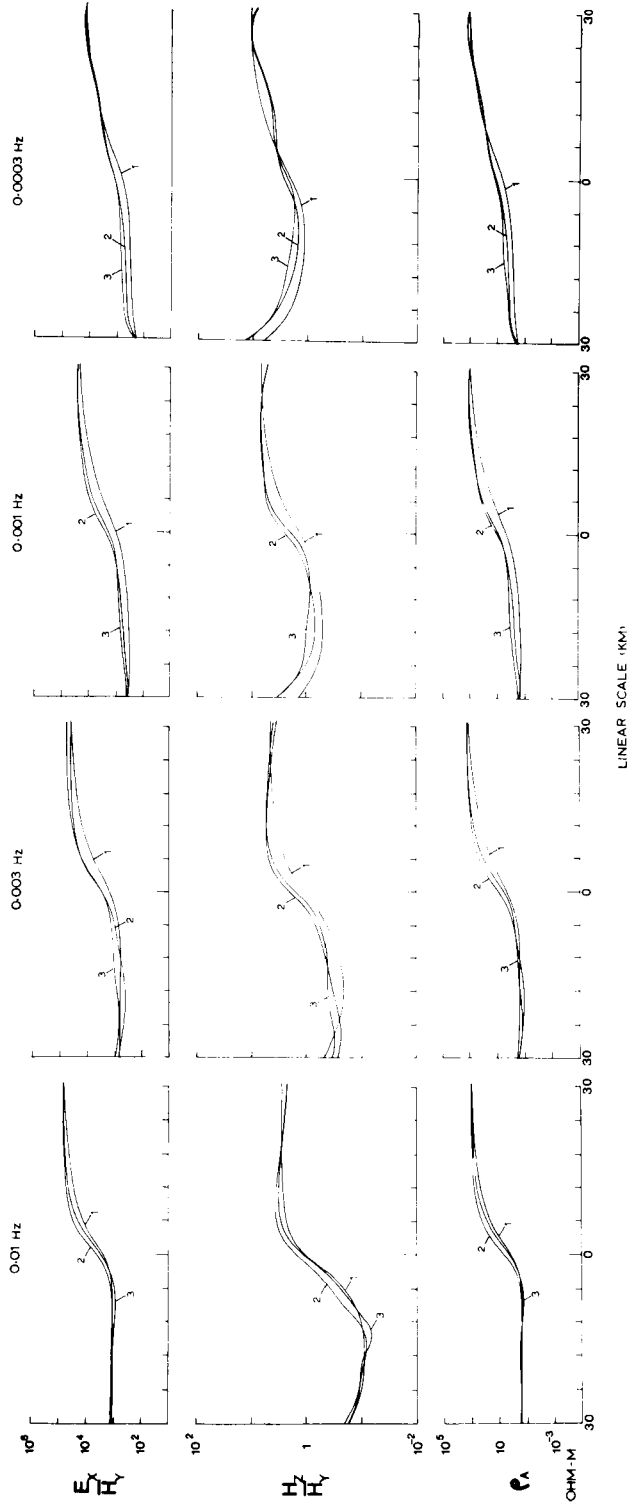
FIG. 4. E-polarization. E_x/H_y, H_z/H_y, and ρ_A for the (1) vertical, (2) step, and (3) shelf models.
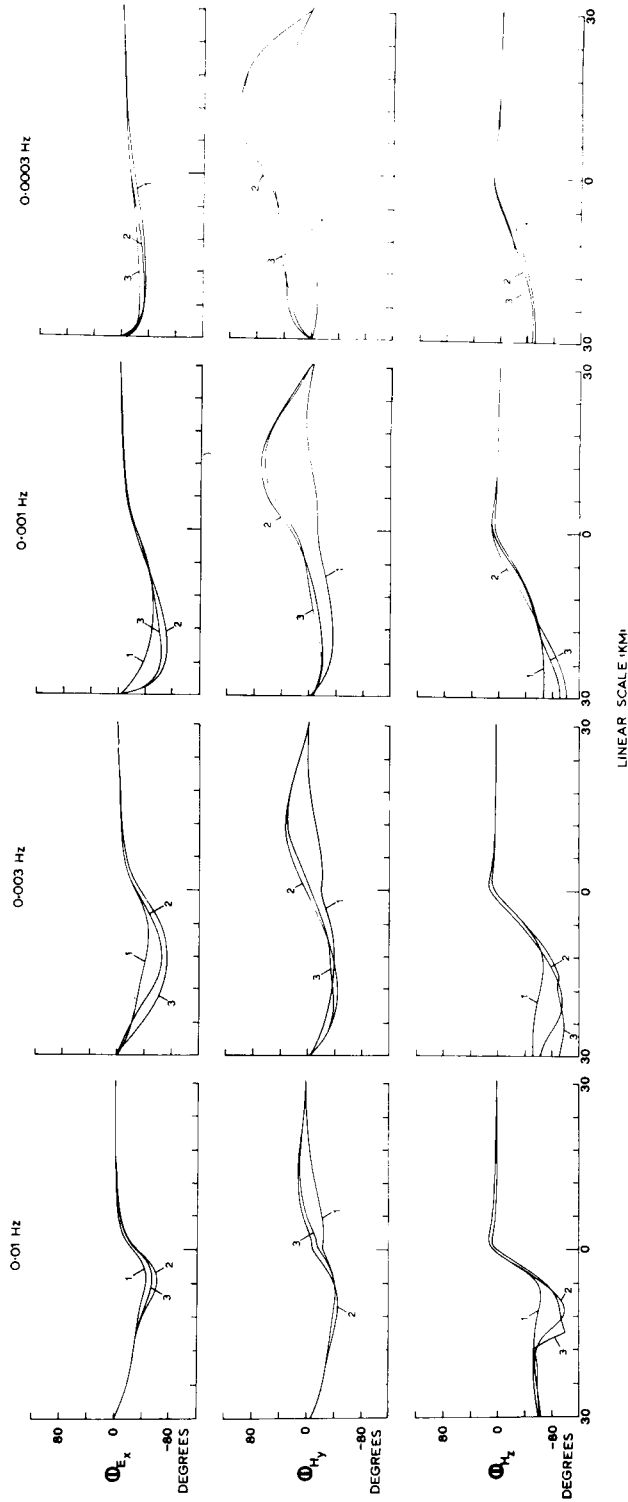
Fig. 5. E-polarization. The phases of $E_x(\phi_{Ex})$, $H_y(\phi_{Hy})$, and $H_z(\phi_{Hz})$ in degrees across the surfaces of the (1) vertical, (2) step, and (3) shelf models.

DISCUSSION OF RESULTS

We observe a fundamental difference between the two polarity cases. The apparent resistivity calculated for the H-polarization case across the contact between the two conductivity regions varies rapidly near the contact and is discontinuous. This is due to a buildup of charge at the interface. Dosso (1966) exhibits a rapidly changing E component near the edge of his wedge and block model in analog studies of variations near a coastline. The behavior Dosso found is similar to the effect in E_y obtained here and would lead to a similar variation in the apparent resistivity. For the E-polarization case, E_x and the apparent resistivity change continuously near the contacts. The curves for E_x, H_y, and H_z are similar to those obtained by Dosso for his E-polarization case.

It is clearly of interest to study the H-polarization case and variations near lateral inhomogeneities, but for accuracy in interpretation of apparent resistivity values near the interfaces between two media of different conductivity, the E-polarization case is more suitable. If, in field measurements, the strike of the feature under investigation can be determined, it is clear that resistivity values calculated from measurements of magnetic field perpendicular to the strike and electric field parallel to the strike will be most directly useful.

REFERENCES

Dosso, H. W., 1966, Analogue model measurements for electromagnetic variations near a coastline: Can. J. Phys., v. 3, p. 917.

Jones, F. W., and Price, A. T., 1969, The perturbation of an alternating field by a conductivity anomaly: IAGA Bulletin No. 26, Abstract III-106, p. 196.

———— 1970a, The perturbations of alternating geomagnetic fields by conductivity anomalies: Geophys. J.R.A.S. v. 20, p. 317.

———— 1970b, The geomagnetic effects of two-dimensional conductivity inhomogeneities at different depths: Geophs. J. Roy. Astr. Soc., In press.